

09,04

Structural and spectral characteristics of  $\text{Pr}_{1-x}\text{Lu}_x\text{BO}_3$  orthoborates

© S.Z. Shmurak, V.V. Kedrov, A.P. Kiselev, T.N. Fursova, I.I. Zver'kova

Osipyan Institute of Solid State Physics RAS,  
Chernogolovka, Russia

E-mail: shmurak@issp.ac.ru

Received December 27, 2021

Revised December 27, 2021

Accepted December 28, 2021

The structure, IR absorption and luminescence spectra of  $\text{Pr}_{0.99-x}\text{Lu}_x\text{Eu}_{0.01}\text{BO}_3$  orthoborates synthesized at  $970^\circ\text{C}$  were studied at  $0 \leq x \leq 0.99$ . An increase in the concentration of lutetium leads to a sequential change of the structural state of the orthoborates. At first, the orthoborates are single-phase and have an aragonite structure ( $0 \leq x \leq 0.1$ ). Then, they become two-phase and contain the aragonite and vaterite phases ( $0.1 < x < 0.6$ ). With a further increase in  $x$  ( $0.6 < x \leq 0.8$ ), the compounds are single-phase with a vaterite structure, then they contain the vaterite and calcite phases ( $0.8 < x \leq 0.95$ ), and, finally, they become single-phase with a calcite structure ( $0.95 < x \leq 0.99$ ). An unambiguous correspondence between the structural modification and IR spectra of these compounds was established. It is shown that the emission of  $\text{Eu}^{3+}$  ions is observed in samples where the concentration of europium exceeds that of praseodymium.

**Keywords:** rare earth orthoborates, X-ray diffraction analysis, crystal structure, IR spectroscopy, luminescence spectra.

DOI: 10.21883/PSS.2022.04.53503.265

## 1. Introduction

Spectral characteristics of orthoborates, doped with optically active rare-earth ions ( $\text{Eu}^{3+}$ ,  $\text{Tb}^{3+}$ ,  $\text{Ce}^{3+}$ ), depend on the sample's structural state [1–4], therefore the study of methods for targeted change of their structure is of considerable interest. It was shown in [5] that the solid solution  $\text{Lu}_{1-x}\text{In}_x\text{BO}_3$ , consisting of lutetium borate ( $\text{LuBO}_3$ ) having two stable structural modifications, vaterite and calcite [6–8], and indium borate ( $\text{InBO}_3$ ) having only one structural modification — calcite [9–11] synthesized at  $780^\circ\text{C}$  (existence temperature of vaterite  $\text{LuBO}_3$ ) with  $x > 0.08$ –0.1 crystallizes in the calcite structure. At the same time,  $\text{Lu}_{1-x}\text{RE}_x\text{BO}_3$  solid solutions ( $\text{RE} = \text{Eu}, \text{Gd}, \text{Tb}, \text{Dy}$  and  $\text{Y}$ ), consisting of lutetium borate and  $\text{REBO}_3$ , having only one structural modification — vaterite [6–8], with  $x > 0.15$ –0.2, synthesized at  $T = 970$ – $1100^\circ\text{C}$  (existence temperature of calcite phase  $\text{LuBO}_3$ ), crystallize in the vaterite structure [12–15].

An increased concentration of  $\text{In}^{3+}$  ions in  $\text{Lu}_{0.98-x}\text{In}_x\text{Eu}_{0.02}\text{BO}_3$  orthoborates synthesized at  $780^\circ\text{C}$  leads to an increase of the calcite phase: with  $0 \leq x < 0.03$  the solid solution has a vaterite structure, a calcite phase occurs at  $0.03 \leq x \leq 0.08$  along with vaterite, while with  $x > 0.08$ –0.1 the compound has a calcite structure. The samples' morphology changes along with structural transformations. Vaterite microcrystals (with  $0 \leq x < 0.03$ ) have a size of  $\sim 0.3$ – $1 \mu\text{m}$ . When indium concentration increases, larger microcrystals sized  $\sim 3 \mu\text{m}$  appear along with smaller ones ( $0.3$ – $1 \mu\text{m}$ ). Quantity of large microcrystals increases with an increase of the calcite phase share. The samples of  $\text{In}_{0.98}\text{Eu}_{0.02}\text{BO}_3$  with

a calcite structure have well-faceted microcrystals sized  $3$ – $5 \mu\text{m}$  [11].

An increased concentration of RE in  $\text{Lu}_{0.99-x}\text{RE}_x\text{Eu}_{0.01}\text{BO}_3$  ( $\text{RE} = \text{Gd}, \text{Eu}, \text{Tb}, \text{Y}$ ) orthoborates synthesized at  $970^\circ\text{C}$  leads to a successive change of their structure: with  $0 \leq x \leq 0.05$ –0.1 the solid solution of orthoborates is single-phase and has a calcite structure (space group  $R\bar{3}c$ ); with  $0.05$ – $0.1 < x \leq 0.1$ –0.25 a vaterite phase (space group  $C2/c$ ) forms along with the calcite structure, while with  $x > 0.1$ –0.25 the solid solution is single-phase with a vaterite structure (space group  $C2/c$ ) [12–15]. Morphology of orthoborate microcrystals changes simultaneously with the structure. Microcrystals of the calcite modification have a size of  $15$ – $20 \mu\text{m}$ . Small microcrystals ( $1$ – $2 \mu\text{m}$ ), number of which increases with increase of  $x$ , form (along with large ones) in the concentration interval  $\text{RE } 0.05$ – $0.1 < x \leq 0.1$ –0.25 where the samples are two-phase. With  $x > 0.1$ –0.25 there are chiefly microcrystals sized  $1$ – $2 \mu\text{m}$  with a vaterite structure.

Papers [11–15] were dedicated to the study of solid solutions of lutetium borate having two structural modifications (vaterite and calcite) and borates having only one modification of lutetium borate: either calcite ( $\text{InBO}_3$ ) or vaterite ( $\text{REBO}_3$ ,  $\text{RE} = \text{Eu}, \text{Gd}, \text{Tb}, \text{Dy}, \text{Y}$ ). Paper [16] describes the structural state of the solid solution of  $\text{LuBO}_3$ , synthesized at  $970^\circ\text{C}$ , and lanthanum orthoborate ( $\text{LaBO}_3$ ) whose structure is neither calcite nor vaterite. The  $\text{LaBO}_3$  compound has two phase states: the low-temperature orthorhombic aragonite phase (space group  $Pnma$ ) and the high-temperature monoclinic phase (space group  $P2_1/m$ ), to which  $\text{LaBO}_3$  changes over at  $1488^\circ\text{C}$  [6,17].  $\text{La}^{3+}$  ions

in the aragonite structure are surrounded by nine oxygen ions, while boron ions have a trigonal coordination by oxygen [18–25]. It should be noted that  $\text{Lu}^{3+}$  ions in the calcite structure, e.g. in  $\text{LuBO}_3$ , are surrounded by six oxygen ions, while boron atoms have, like the aragonite, a trigonal coordination by oxygen —  $(\text{BO}_3)^{3-}$  [26]. At the same time,  $\text{Lu}^{3+}$  ions in the vaterite structure are surrounded by eight oxygen ions, while three boron atoms with a tetrahedral environment by oxygen make up a group  $(\text{B}_3\text{O}_9)^{9-}$  in the form of a three-dimensional ring [27,28].

The following might be anticipated as a result of synthesis (at  $T = 970^\circ\text{C}$ ) of a solid solution of  $\text{LaBO}_3$  orthoborate, which has an aragonite structure at this temperature, and  $\text{LuBO}_3$  which has a calcite structure at  $T = 970^\circ\text{C}$ : the  $\text{La}_{1-x}\text{Lu}_x\text{BO}_3$  compound, with an increase of the  $\text{Lu}^{3+}(x)$  concentration, will have an aragonite structure first, and then a calcite phase will arise along with the aragonite structure, and the compound will have a calcite structure with a subsequent increase of  $x$ . However, as shown in [16], a different sequence of structural state alternation is observed in the  $\text{La}_{0.98-x}\text{Lu}_x\text{Eu}_{0.02}\text{BO}_3$  compound with increase of  $x$ . With  $0 \leq x \leq 0.1$  the compounds are single-phase and have an aragonite structure. With  $0.15 \leq x \leq 0.8$  the samples of  $\text{La}_{0.98-x}\text{Lu}_x\text{Eu}_{0.02}\text{BO}_3$  are two-phase, they contain aragonite and vaterite phases. With  $0.8 < x < 0.88$  the orthoborates have a vaterite structure (space group  $P6_3/mmc$ ). With  $0.88 < x < 0.93$  the samples of  $\text{La}_{0.98-x}\text{Lu}_x\text{Eu}_{0.02}\text{BO}_3$  are two-phase, they contain vaterite and calcite phases. Finally, with  $0.93 \leq x \leq 0.98$  the orthoborates are single-phase and have a calcite structure (space group  $R\bar{3}c$ ). Thus, when the  $\text{Lu}^{3+}$  concentration in  $\text{La}_{0.98-x}\text{Lu}_x\text{Eu}_{0.02}\text{BO}_3$  compounds synthesized at  $970^\circ\text{C}$  increases, a vaterite phase first forms along with an aragonite phase, despite the fact that the  $\text{LuBO}_3$  orthoborate synthesized at  $T = 970^\circ\text{C}$  has a calcite structure. A calcite phase stable at the given temperature arises, along with the vaterite structure, only with  $x > 0.88$ . It should be noted that 2 at.%  $\text{Eu}^{3+}$  in  $\text{La}_{0.98-x}\text{Lu}_x\text{Eu}_{0.02}\text{BO}_3$  compounds were used as an optically active and structure sensitive label and did not significantly affect the sample structure.

With an increase of  $\text{Lu}^{3+}(x)$  concentration, a vaterite phase forms in the samples of  $\text{La}_{0.98-x}\text{Lu}_x\text{Eu}_{0.02}\text{BO}_3$  (which initially have an aragonite structure), like in the samples of  $\text{Lu}_{1-x}\text{RE}_x\text{BO}_3$  ( $\text{RE} = \text{Eu}, \text{Gd}, \text{Tb}, \text{Dy}$  and  $\text{Y}$ ), in the sample bulk first, and then a vaterite structure forms in the entire sample. At the same time, a calcite phase (with  $0.88 < x < 0.93$ ) in  $\text{La}_{0.98-x}\text{Lu}_x\text{Eu}_{0.02}\text{BO}_3$  orthoborates with the vaterite structure forms in the sample's near-surface regions first, and then a calcite structure forms in the entire sample, like in the samples of  $\text{Lu}_{0.98-x}\text{In}_x\text{Eu}_{0.02}\text{BO}_3$ .

It is important to determine the commonness of the structure rearrangement observed in the samples of  $\text{La}_{0.98-x}\text{Lu}_x\text{Eu}_{0.02}\text{BO}_3$  with an increase of  $\text{Lu}^{3+}$  ions concentration. It is known that, along with  $\text{LaBO}_3$ , the Pr and Nd orthoborates synthesized at  $T = 970^\circ\text{C}$  also have an aragonite structure [6,29–31]. The present paper is

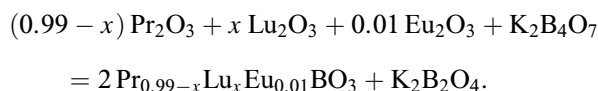
dedicated to revealing changes of the structure, morphology, IR absorption spectra of  $\text{Pr}_{0.99-x}\text{Lu}_x\text{Eu}_{0.01}\text{BO}_3$  solid solutions with  $0 \leq x \leq 0.99$ .

Praseodymium orthoborate  $\text{PrBO}_3$ , like lanthanum orthoborate  $\text{LaBO}_3$ , has two phase states: a low-temperature orthorhombic aragonite phase ( $\lambda\text{-PrBO}_3$ ) (space group  $Pnma$ ) and a high-temperature triclinic phase  $\nu\text{-PrBO}_3$  (space group  $P-1$ ), two which  $\text{PrBO}_3$  changes over at  $1500^\circ\text{C}$  [6,29–31].  $\text{Pr}^{3+}$  ions in the aragonite structure ( $\lambda\text{-PrBO}_3$ ), like  $\text{La}^{3+}$  ions in  $\text{LaBO}_3$ , are surrounded by nine oxygen ions, while boron ions have a trigonal coordination by oxygen  $(\text{BO}_3)^{3-}$  [29–31].

## 2. Experimental procedures

### 2.1. Sample synthesis

Samples of orthoborate polycrystalline powders of composition  $\text{Pr}_{0.99-x}\text{Lu}_x\text{Eu}_{0.01}\text{BO}_3$  were obtained by interaction of oxides of rare earth elements with molten potassium tetraborate according to the reaction:



The potassium tetraborate amount taken for the reaction provided a 10–20% excess of the boron-containing reagent in relation to the stoichiometric amount. The initial compounds for orthoborate synthesis were potassium tetraborate tetrahydrate  $\text{K}_2\text{B}_4\text{O}_7 \cdot 4\text{H}_2\text{O}$  and calibrated aqueous solutions of nitrates of rare earth elements. All the used chemical substances were „analytical reagent grade“.

Microcrystalline orthoborate powders were synthesized as follows. A weighed amount of potassium tetraborate tetrahydrate was placed in a ceramic cup, stoichiometric amounts of aqueous solutions of rare earth nitrates, taken in the required ratio, were added and thoroughly mixed. The obtained aqueous suspension was heated on a hot plate and water was driven off under weak boiling. The obtained solid solution was annealed at  $550^\circ\text{C}$  for 20 min to remove water and nitrate decomposition products, and then thoroughly ground in an agate mortar. The obtained powder was transferred into a ceramic crucible and subjected to high-temperature annealing at  $T = 970^\circ\text{C}$  for 2 h. The annealing product was treated with aqueous solution of hydrochloric acid with the concentration of 5 wt.% for 0.2 h while constantly mixing on a magnetic mixer. Orthoborate polycrystals were isolated by filtering the obtained aqueous suspension, followed by washing with water, alcohol, and product drying on a filter. The obtained powders of orthoborate polycrystals were finally dried in air at  $T = 200^\circ\text{C}$  for 0.5 h.

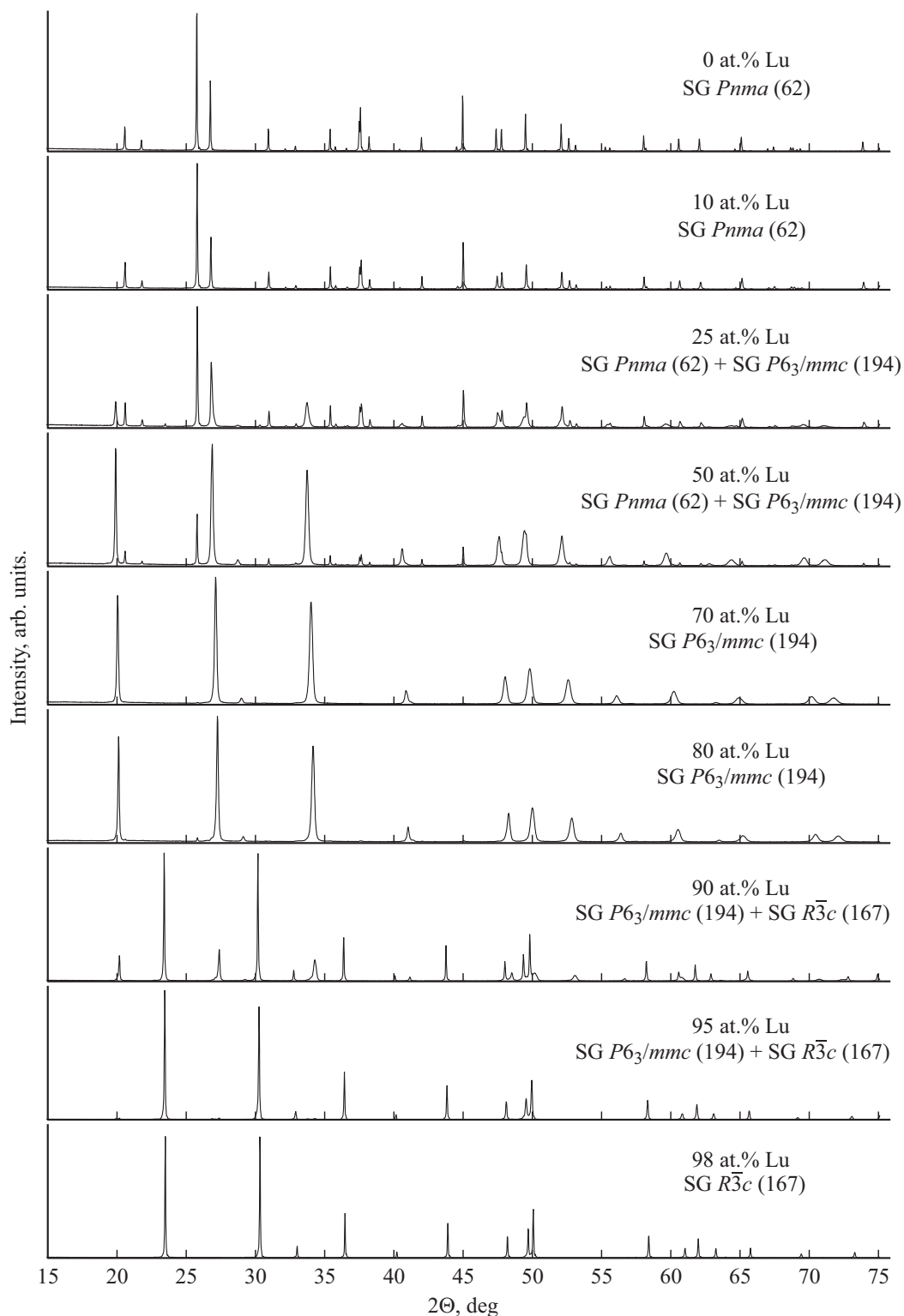


**Figure 1.** Diffraction pattern for samples of  $\text{Pr}_{0.99-x}\text{Lu}_x\text{Eu}_{0.01}\text{BO}_3$  ( $0 \leq x \leq 0.99$ ).

## 2.2. Research methods

X-ray diffraction studies were performed using a Rigaku SmartLab SE diffractometer with  $\text{CuK}\alpha$  radiation,  $\lambda = 1.54178 \text{ \AA}$ , 40 kV, 35 mA. Angular interval

$2\theta = 10\text{--}140^\circ$ . Phase analysis of the samples and calculation of lattice parameters were performed using the Match and PowderCell 2.4 programs.

The IR spectra of the samples were measured in a VERTEX 80v Fourier-spectrometer in the spectral range

**Table 1.** Content of aragonite (A), vaterite (B) and calcite (K) phases in samples of  $\text{Pr}_{1-x-y-z}\text{Lu}_x\text{Eu}_y\text{Tb}_z\text{BO}_3$ 

Concentration RE, at.%				A, %	$V_A,$ $\text{\AA}^3$	B, %	$V_B,$ $\text{\AA}^3$	K, %	$V_K,$ $\text{\AA}^3$
Pr	Lu	Eu	Tb						
99	0	1	0	100	118.6	0	—	0	—
89	10	1	0	100	118.4	0	—	0	—
74	25	1	0	67	118.2	33	112.1	0	—
49	50	1	0	19	118.2	81	111.9	0	—
29	70	1	0	0	—	100	109.8	0	—
19	80	1	0	0	—	100	108.1	0	—
9	90	1	0	0	—	31	106.4	69	114.6
4	95	1	0	0	—	2	—	98	114.0
1	98	1	0	0	—	0	—	100	113.2
0	99	1	0	0	—	0	—	100	113.1
1	97	2	0	0	—	0	—	100	113.3
1	96	3	0	0	—	0	—	100	113.5
2	96	0	2	0	—	0	—	100	113.5
2	94	0	4	0	—	0	—	100	113.6

Note.  $V_A$  — volume of aragonite unit cell reduced to  $Z = 2$ ,  $V_B$  — volume of vaterite unit cell,  $Z = 2$ ,  $V_K$  — volume of calcite unit cell reduced to  $Z = 2$ .

of  $400\text{--}5000\text{ cm}^{-1}$ , resolution being  $2\text{ cm}^{-1}$ . For measurements, the polycrystal powders were ground in an agate mortar, and then were applied in a thin layer onto a crystalline polished substrate KBr.

The sample morphology was studied using a Supra 50VP X-ray microanalyzer with an add-on for EDS INCA (Oxford).

Photoluminescence spectra and luminescence excitation spectra were studied on a unit that consisted of a light source — DKSSh-150 lamp, two MDR-4 and MDR-6 monochromators (spectral range  $200\text{--}1000\text{ nm}$ , dispersion  $1.3\text{ nm/mm}$ ). Luminescence was recorded by means of photomultiplier FEU-106 (spectral sensitivity range  $200\text{--}800\text{ nm}$ ) and an amplification system. The MDR-4 monochromator was used for studying the luminescence excitation spectra of the samples, the MDR-6 monochromator was used for studying luminescence spectra. Spectral and structural characteristics, as well as the morphology of the samples were studied at room temperature.

### 3. X-ray diffraction studies

Diffraction patterns for the powder sample of  $\text{Pr}_{0.99-x}\text{Lu}_x\text{Eu}_{0.01}\text{BO}_3$  orthoborates are shown in Fig. 1. The phase composition of the studied compounds and unit cell volumes are given in Table 1.

The  $\text{Pr}_{0.99-x}\text{Lu}_x\text{Eu}_{0.01}\text{BO}_3$  orthoborates with  $0 \leq x \leq 0.1$  are single-phase and have an aragonite structure ( $\text{PrBO}_3$ , PDF 01-079-8645) —  $Pnma$  (space group № 62),  $Z = 4$ . The samples are two-phase in the interval  $0.1 < x < 0.6$  — along with aragonite, they contain a vaterite phase (PDF 74-1938) —  $P6_3/mmc$  (space group № 194),  $Z = 2$ . The samples have a vaterite structure in the interval  $0.6 < x \leq 0.8$ . With  $x > 0.8$ , a calcite phase, space group ( $R\bar{3}c$ ) № 167 (PDF 72-1053),  $Z = 6$ , amount

of which increases with increase of  $\text{Lu}^{3+}$  concentration, is observed along with the vaterite. The samples in the concentration interval  $0.8 < x \leq 0.95$  are two-phase and contain vaterite and calcite phases. With  $x > 0.95$  the samples are single-phase with a calcite structure.

The unit cell volume monotonically decreases with an increase of  $\text{Lu}^{3+}$  ions concentration, in the interval  $0 \leq x \leq 0.1$  in single-phase samples having an aragonite structure. This indicates a substitution of  $\text{Pr}^{3+}$  ions, having the ionic radius of  $1.052\text{ \AA}$ , with  $\text{Lu}^{3+}$  ions having a considerably smaller ionic radius ( $0.867\text{ \AA}$ ) [32]. The maximum possible dissolution of  $\text{Lu}^{3+}$  ions in the aragonite phase  $\text{Pr}_{0.99}\text{Eu}_{0.01}\text{BO}_3$  is  $\sim 10\text{ at.}\%$  (Fig. 2, 3). The composition of the forming solid solution is  $\sim \text{Pr}_{0.89}\text{Lu}_{0.1}\text{Eu}_{0.01}\text{BO}_3$ . In

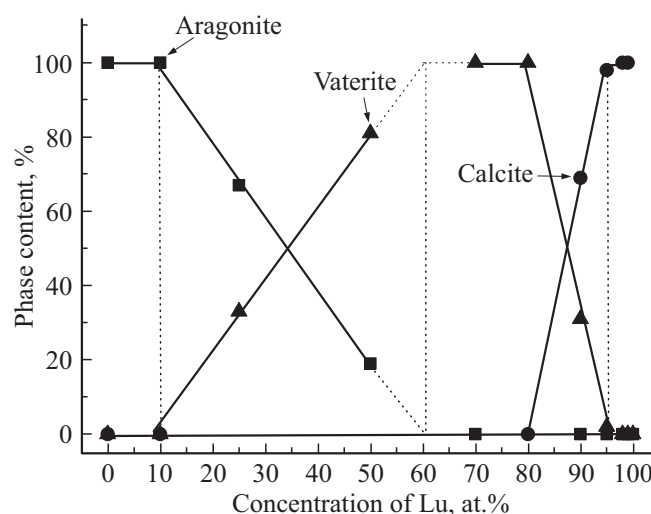


**Figure 2.** Phase composition of the synthesized samples of  $\text{Pr}_{0.99-x}\text{Lu}_x\text{Eu}_{0.01}\text{BO}_3$  depending on Lu concentration in the charge: a square — aragonite, a triangle — vaterite, a circle — calcite.

**Table 2.** Regions of Pr and La concentrations where certain structural states of  $\text{Pr}_{0.99-x}\text{Lu}_x\text{Eu}_{0.01}\text{BO}_3$  and  $\text{La}_{0.98-x}\text{Lu}_x\text{Eu}_{0.02}\text{BO}_3$  orthoborates exist

Compound	Values of $x$ at which the given structures exist				
	Aragonite ( $Pnma$ )	Aragonite + Vaterite	Vaterite ( $P6_3/mmc$ )	Vaterite + calcite	Calcite ( $R\bar{3}c$ )
$\text{Pr}_{0.99-x}\text{Lu}_x\text{Eu}_{0.01}\text{BO}_3$	$0 \leq x \leq 0.1$	$0.1 < x < 0.6$	$0.6 < x \leq 0.8$	$0.8 < x \leq 0.95$	$0.95 < x \leq 0.99$
$^1\text{La}_{0.98-x}\text{Lu}_x\text{Eu}_{0.02}\text{BO}_3$	$0 \leq x < 0.15$	$0.15 \leq x \leq 0.8$	$0.8 < x < 0.88$	$0.88 \leq x < 0.93$	$0.93 \leq x \leq 0.98$

Note. <sup>1</sup> — The data of [16].

the course of subsequent doping, the additional lutetium does not make part of the aragonite structure but is consumed for increase of the vaterite phase amount.

The volumes of the unit cells of the aragonite and vaterite phases in the two-phase aragonite–vaterite region, with  $0.1 < x < 0.6$ , remain virtually constant (Fig. 3). The approximate composition of the vaterite phase, estimated along the boundary of vaterite unit cell volume change is  $\text{Pr}_{0.4}\text{Lu}_{0.59}\text{Eu}_{0.01}\text{BO}_3$ . As seen from Fig. 2, the ratio between aragonite and vaterite phases changes in the concentration interval  $0.1 < x < 0.6$ . Only the calcite phase whose unit cell volume decreases with increase of  $x$  is observed in the concentration interval  $0.95 < x \leq 0.99$ . Consequently, when  $\text{Lu}_{0.99}\text{Eu}_{0.01}\text{BO}_3$  is doped with  $\text{Pr}^{3+}$  in the concentration range of 0–4 at.%, the calcite unit cell volume increases, which means praseodymium dissolution in the lutetium orthoborate with a calcite structure. The maximum possible dissolution of  $\text{Pr}^{3+}$  ions in the calcite phase is  $\sim 4\text{--}5$  at.% (according to the boundary of unit cell volume change). The composition of the forming solid solution is  $\sim \text{Pr}_{0.05}\text{Lu}_{0.94}\text{Eu}_{0.01}\text{BO}_3$ .

With subsequent increase of praseodymium concentration in  $\text{Lu}_{0.99}\text{Eu}_{0.01}\text{BO}_3$ , in the concentration interval  $0.95 \geq x \geq 0.9$ , the calcite phase is complemented by a

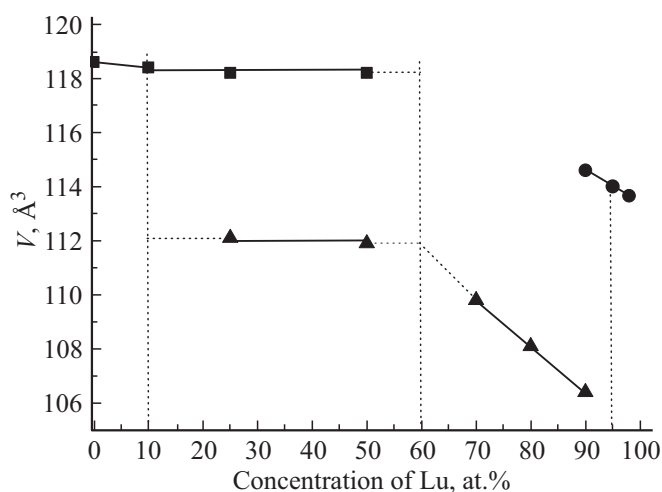


**Figure 3.** Volumes of unit cells of structural modifications  $\text{Pr}_{0.99-x}\text{Lu}_x\text{Eu}_{0.01}\text{BO}_3$  reduced to  $Z = 2$ : a square — aragonite, a triangle — vaterite, a circle — calcite.

vaterite phase whose cell volume increases with an increase of praseodymium content in the charge (i.e. it increases with a decrease of lutetium content), the ratio between the number of vaterite and calcite phases also changes (Table 1, Fig. 2, 3).

The samples in the concentration interval  $0.6 < x \leq 0.8$  are single-phase with a vaterite structure, the whole additional praseodymium amount is dissolved in vaterite and increases the unit cell volume. The limit of  $\text{Pr}^{3+}$  solubility in the vaterite phase is achieved when the concentration of  $\text{Pr}^{3+}$  is  $\sim 39$  at.% (60 at.%  $\text{Lu}^{3+}$ ). Further increase of praseodymium concentration does not lead to a change in the vaterite unit cell volume, but is consumed for increase of aragonite phase amount in the two-phase region with  $0.1 < x < 0.6$ .

Thus, the following conclusions can be made based on the X-ray diffraction studies. Five regions of  $\text{Lu}^{3+}$  concentrations, where certain structural states exist, can be distinguished in  $\text{Pr}_{0.99-x}\text{Lu}_x\text{Eu}_{0.01}\text{BO}_3$  orthoborates, like in  $\text{La}_{0.98-x}\text{Lu}_x\text{Eu}_{0.02}\text{BO}_3$  compounds [16]. As lutetium concentration grows, three types of crystalline phases change successively: aragonite, vaterite and calcite (Table 2). This process can be represented schematically as follows: aragonite (with  $0 \leq x \leq 0.1$ )  $\rightarrow$  aragonite + vaterite ( $0.1 < x < 0.6$ )  $\rightarrow$  vaterite ( $0.6 < x \leq 0.8$ )  $\rightarrow$  vaterite + calcite ( $0.8 < x \leq 0.95$ )  $\rightarrow$  calcite ( $0.95 < x \leq 0.99$ ).

The maximum possible dissolution of  $\text{Lu}^{3+}$  ions in the aragonite phase  $\text{Pr}_{0.99}\text{Eu}_{0.01}\text{BO}_3$  is  $\sim 10$  at.%. The approximate composition of the vaterite phase, according to the boundary of vaterite unit cell volume change, is  $\text{Pr}_{0.39}\text{Lu}_{0.6}\text{Eu}_{0.01}\text{BO}_3$ . The maximum possible dissolution of  $\text{Pr}^{3+}$  ions in the calcite phase is  $\sim 5$  at.%. A low value of  $\text{Pr}^{3+}$  limit solubility in the calcite phase of composition  $\text{Lu}_{0.99}\text{Eu}_{0.01}\text{BO}_3$  is probably due to a large difference in the ionic radii of  $\text{Pr}^{3+}$  and  $\text{Lu}^{3+}$ .

It should be noted that the interval of  $\text{Lu}^{3+}$  concentrations where a vaterite phase exists in  $\text{Pr}_{0.99-x}\text{Lu}_x\text{Eu}_{0.01}\text{BO}_3$  orthoborates ( $0.6 < x \leq 0.8$ ), is much larger than in  $\text{La}_{0.98-x}\text{Lu}_x\text{Eu}_{0.02}\text{BO}_3$  ( $0.8 < x < 0.88$ ) (Table 2).

#### 4. Sample morphology

The samples of  $\text{Pr}_{0.99-x}\text{Lu}_x\text{Eu}_{0.01}\text{BO}_3$  with  $0 \leq x \leq 0.1$ , which have an aragonite structure according to the X-ray

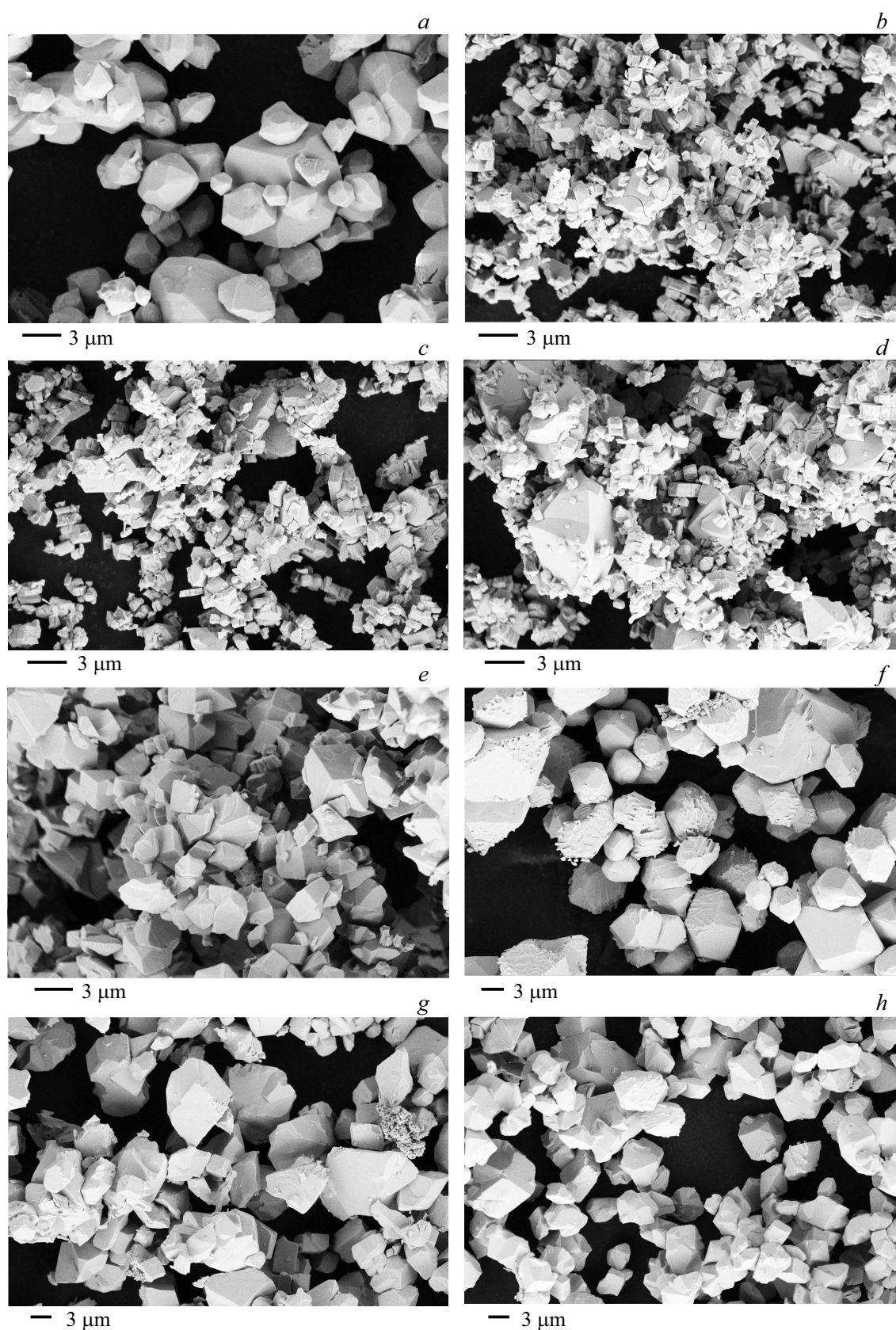


**Figure 4.** Morphology of the samples of  $\text{Pr}_{0.99-x}\text{Lu}_x\text{Eu}_{0.01}\text{BO}_3$ : *a* —  $\text{Pr}_{0.99}\text{Eu}_{0.01}\text{BO}_3$ , *b* —  $\text{Pr}_{0.49}\text{Lu}_{0.5}\text{Eu}_{0.01}\text{BO}_3$ , *c* —  $\text{Pr}_{0.29}\text{Lu}_{0.7}\text{Eu}_{0.01}\text{BO}_3$ , *d* —  $\text{Pr}_{0.09}\text{Lu}_{0.9}\text{Eu}_{0.01}\text{BO}_3$ , *e* —  $\text{Pr}_{0.04}\text{Lu}_{0.95}\text{Eu}_{0.01}\text{BO}_3$ , *f* —  $\text{Lu}_{0.99}\text{Eu}_{0.01}\text{BO}_3$ , *g* —  $\text{Pr}_{0.01}\text{Lu}_{0.97}\text{Eu}_{0.02}\text{BO}_3$ , *h* —  $\text{Pr}_{0.02}\text{Lu}_{0.96}\text{Tb}_{0.02}\text{BO}_3$ .

diffraction analysis data (Table 1), contain microcrystals sized  $\sim 2\text{--}8\ \mu\text{m}$  (Fig. 4, *a*). When concentration of  $\text{Lu}^{3+}$  increases ( $0.25 \leq x \leq 0.7$ ), the samples contain small ( $0.5\text{--}1\ \mu\text{m}$ ) and larger microcrystals ( $3\text{--}5\ \mu\text{m}$ ). According to the X-ray diffraction analysis data, an increased concentration of  $\text{Lu}^{3+}$  ions leads to a decrease of aragonite amount and an increase of the vaterite share (Table 1). As the vaterite phase amount increases, the number of small crystals ( $0.5\text{--}1\ \mu\text{m}$ ) increases (Fig. 4, *b, c*). The samples of  $\text{Pr}_{0.99-x}\text{Lu}_x\text{Eu}_{0.01}\text{BO}_3$  with  $x = 0.7$  and  $0.8$ , containing 100% of vaterite (Table 1), consist of microcrystals sized  $0.5\text{--}3\ \mu\text{m}$  (Fig. 4, *c*). As the  $\text{Lu}^{3+}$  concentration further increases (with  $0.8 < x < 0.95$ ), the number of small microcrystals ( $0.5\text{--}1\ \mu\text{m}$ ) decreases, while that of larger ones ( $\sim 2\text{--}4\ \mu\text{m}$ ) increases (Fig. 4, *d*). A decrease of the vaterite phase amount and an increase of the calcite phase share are observed in this range of  $\text{Lu}^{3+}$  ion concentrations (Table 1). The samples of  $\text{Pr}_{0.04}\text{Lu}_{0.95}\text{Eu}_{0.01}\text{BO}_3$ , containing 98% of calcite, have chiefly microcrystals sized  $\sim 2\text{--}4\ \mu\text{m}$  (Fig. 4, *e*).  $\text{Lu}_{0.99}\text{Eu}_{0.01}\text{BO}_3$  orthoborates with a calcite structure consist of microcrystals sized  $3\text{--}10\ \mu\text{m}$  (Fig. 4, *f*).

Thus, addition of a small number of  $\text{Pr}^{3+}$  ions ( $\sim 5\ \text{at.}\%$ ) to  $\text{Lu}_{0.99}\text{Eu}_{0.01}\text{BO}_3$ , like  $\text{La}^{3+}$  [16], leads to a noticeable change of microcrystal sizes, but does not change the sample structure (Table 1).

Microcrystals sized  $3\text{--}10\ \mu\text{m}$  (Fig. 4, *g*) are observed in  $\text{LuBO}_3$  orthoborates containing 1 at.% Pr, 2 and 3 at.% of Eu, which have a calcite structure (Table 1). The same microcrystals are observed in the  $\text{LuBO}_3$  samples containing 2 at.% of Pr, 2 and 4 at.% of Tb, which also have a calcite structure (Table 1) (Fig. 4, *h*).

The following conclusions can be made based on the morphology study of  $\text{Pr}_{0.99-x}\text{Lu}_x\text{Eu}_{0.01}\text{BO}_3$  with  $0 \leq x \leq 0.99$ . With the synthesis method used here, the samples having an aragonite structure consist of microcrystals sized  $\sim 2\text{--}8\ \mu\text{m}$  (Fig. 4, *a*).  $\text{Pr}_{0.29}\text{Lu}_{0.7}\text{Eu}_{0.01}\text{BO}_3$  and  $\text{Pr}_{0.19}\text{Lu}_{0.8}\text{Eu}_{0.01}\text{BO}_3$  orthoborates (100% of vaterite) consist of microcrystals sized  $\sim 0.5\text{--}3\ \mu\text{m}$  (Fig. 4, *c*). It should be noted that the  $\text{Lu}_{1-x}\text{RE}_x\text{BO}_3$  compounds ( $\text{RE} = \text{Eu, Gd, Tb}$ ), obtained by the same method and having a vaterite structure, consist of microcrystals sized ( $\sim 1\text{--}2\ \mu\text{m}$ ) [23,24]. The  $\text{Pr}_{0.99-x}\text{Lu}_x\text{Eu}_{0.01}\text{BO}_3$  ( $0.95 \leq x \leq 0.99$ ) compounds with a calcite structure consist of microcrystals whose sizes with  $x = 0.95$  and  $0.99$  are equal to  $\sim 2\text{--}4$  and  $\sim 3\text{--}10\ \mu\text{m}$  respectively (Fig. 4, *e, f*).

## 5. Results of IR spectroscopy

It is known that borates of rare earth elements with the general formula  $\text{REBO}_3$  ( $\text{RE} = \text{La}\text{--}\text{Lu}$ ) are characterized by structures with complex anions, formed by flat trigonal groups  $\text{BO}_3$  or tetrahedrons  $\text{BO}_4$ , or by  $\text{BO}_3$  and  $\text{BO}_4$  groups simultaneously [26]. The  $\text{PrBO}_3$  compound in the orthoborate series pertains to the structural type of aragonite, in whose crystal lattice the anions  $(\text{BO}_3)^{3-}$  are flat trigonal groups. Fig. 5 gives the IR absorption spectra for the

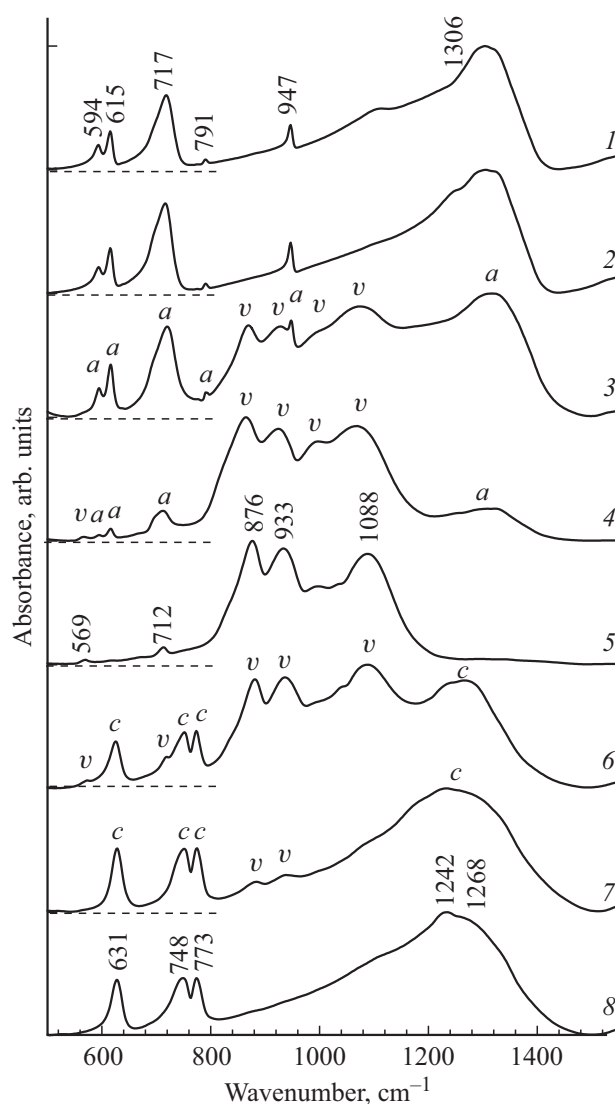


**Figure 5.** IR spectra of  $\text{Pr}_{0.99-x}\text{Lu}_x\text{Eu}_{0.01}\text{BO}_3$  orthoborates: 1 —  $\text{Pr}_{0.99}\text{Eu}_{0.01}\text{BO}_3$ , 2 —  $\text{Pr}_{0.89}\text{Lu}_{0.1}\text{Eu}_{0.01}\text{BO}_3$ , 3 —  $\text{Pr}_{0.74}\text{Lu}_{0.25}\text{Eu}_{0.01}\text{BO}_3$ , 4 —  $\text{Pr}_{0.49}\text{Lu}_{0.5}\text{Eu}_{0.01}\text{BO}_3$ , 5 —  $\text{Pr}_{0.19}\text{Lu}_{0.8}\text{Eu}_{0.01}\text{BO}_3$ , 6 —  $\text{Pr}_{0.09}\text{Lu}_{0.9}\text{Eu}_{0.01}\text{BO}_3$ , 7 —  $\text{Pr}_{0.04}\text{Lu}_{0.95}\text{Eu}_{0.01}\text{BO}_3$ , 8 —  $\text{Pr}_{0.01}\text{Lu}_{0.98}\text{Eu}_{0.01}\text{BO}_3$ . The zero values of ordinate axes for the spectra 1–7 are showed by a dashed line.

$\text{Pr}_{0.99-x}\text{Lu}_x\text{Eu}_{0.01}\text{BO}_3$  compounds with  $0 \leq x \leq 0.98$  in the frequency range of vibrations of B–O-bonds. The spectrum for the sample of composition  $\text{Pr}_{0.99}\text{Eu}_{0.01}\text{BO}_3$  (Fig. 5, spectrum 1) contains absorption bands 594, 615, 717, 791, 947 and  $1306\ \text{cm}^{-1}$ . The absorption spectrum for  $\text{Pr}_{0.99}\text{Eu}_{0.01}\text{BO}_3$  (Fig. 5, spectrum 1) is similar to the spectrum for  $\text{PrBO}_3$  with an aragonite structure given in [30,33]. An analysis of vibrations of planar ions  $(\text{BO}_3)^{3-}$ , performed in [26], makes it possible to classify the absorption bands 594, 615 and doublet 717,  $791\ \text{cm}^{-1}$  as bending vibrations  $\nu_4$  and  $\nu_2$ , respectively, while the absorption bands 947 and  $1306\ \text{cm}^{-1}$  — as stretching vibrations  $\nu_1$  and  $\nu_3$  of B–O bonds respectively.

The IR spectra for the samples of  $Pr_{0.99}Eu_{0.01}BO_3$  and  $Pr_{0.89}Lu_{0.1}Eu_{0.01}BO_3$  (Fig. 5, spectra 1 and 2) coincide. According to the X-ray diffraction analysis data, both samples have an aragonite structure (Table 1). Along with the aragonite phase, additional bands „*v*“ (Fig. 5, spectra 3, 4) appear in the spectra of  $Pr_{0.99-x}Lu_xEu_{0.01}BO_3$  samples with an increase in the Lu concentration at  $0.25 \leq x \leq 0.8$ . Their intensity increases with increase of the Lu concentration, while intensity of the bands of the aragonite phase „*a*“ decreases. The absorption spectrum for the sample of  $Pr_{0.19}Lu_{0.8}Eu_{0.01}BO_3$  (Fig. 5, spectrum 5) has a group of intensive absorption bands in the range of  $800\text{--}1200\text{ cm}^{-1}$  with the maxima at 876, 933, and  $1088\text{ cm}^{-1}$ , as well as weak absorption bands  $569$  and  $712\text{ cm}^{-1}$ . No aragonite phase lines are observed in the spectrum, the spectrum is similar to the spectrum for the sample of  $La_{0.1}Lu_{0.88}Eu_{0.02}BO_3$  with a vaterite structure [16]. The vibrational spectrum of borates in a vaterite structure differs considerably from their spectra in an aragonite and calcite structure. This is due to the tetragonal coordination of boron atoms with the formation of an anion  $(B_3O_9)^{9-}$  in the form of a three-dimensional ring in this structure. The absorption band of stretching vibrations of B–O-bonds in a vaterite structure is in the range of  $800\text{--}1200\text{ cm}^{-1}$ , while in aragonite and calcite structures with a trigonal environment of boron atoms it is in the range of  $1200\text{--}1400\text{ cm}^{-1}$  [26,33,34]. According to the X-ray phase analysis data, the sample of  $Pr_{0.19}Lu_{0.8}Eu_{0.01}BO_3$  is single-phase and has a vaterite structure (Table 1).

With subsequent increase of  $Lu^{3+}$  concentration ( $0.8 < x \leq 0.98$ ), additional bands „*c*“ (Fig. 5, spectra 6–8) appear in the IR spectra of the  $Pr_{0.99-x}Lu_xEu_{0.01}BO_3$  compounds in addition to the absorption bands of the vaterite phase „*v*“. The spectrum for the sample of  $Pr_{0.01}Lu_{0.98}Eu_{0.01}BO_3$  has only the absorption bands  $631$ ,  $748$ ,  $773$  and  $1242$  with a shoulder  $\sim 1260\text{ cm}^{-1}$  (Fig. 5, spectrum 8), corresponding to the calcite structure spectrum [13,26]. The absorption bands  $631$ ,  $748$ ,  $773\text{ cm}^{-1}$  due to bending vibrations, while the band with the maximum of  $1242\text{ cm}^{-1}$  — by stretching vibrations of B–O bonds.

Thus, the study of the IR spectra has shown that an increase of  $Lu^{3+}$  concentration in the  $Pr_{0.99-x}Lu_xEu_{0.01}BO_3$  system ( $0 \leq x \leq 0.98$ ) leads to a change of the IR spectra of the samples according to the sequence of change of their phase composition (Tables 1 and 2): aragonite  $\rightarrow$  aragonite + vaterite  $\rightarrow$  vaterite  $\rightarrow$  vaterite + calcite  $\rightarrow$  calcite.

## 6. Luminescence spectra and luminescence excitation spectra

Luminescence is not observed in  $Pr_{0.99-x}Lu_xEu_{0.01}BO_3$  orthoborates with  $0 \leq x \leq 0.98$  in the studied wavelength range of  $350\text{--}800\text{ nm}$ . A possible reasons of luminescence absence in these compounds is due to the fact that a charge transfer from  $Pr^{3+}$  to  $Eu^{3+}$  takes place

in praseodymium- and europium-containing borates as follows:  $Pr^{3+} + Eu^{3+} \rightarrow Pr^{4+} + Eu^{2+}$ . This process is possible since praseodymium may have the valency 3+ and 4+, while europium may have the valency 2+ and 3+ [32]. A charge transfer from  $Ce^{3+}$  ions to  $Eu^{3+}$  ions (metal–metal charge transfer (MMCT)) according to the scheme  $Ce^{3+} + Eu^{3+} \rightarrow Ce^{4+} + Eu^{2+}$  was previously observed in pioneering papers [35,36] in a number of compounds, including cerium- and europium-doped borates. A charge transfer from one activator to another leads to quenching of luminescence of the activators involved in this process.

When stoichiometry of charge transfer from praseodymium to europium is implemented, the number of  $Eu^{3+}$  ions with quenched luminescence must be equal to the number of  $Pr^{3+}$  ions. Therefore, if concentration of europium ions in a sample exceeds the concentration of praseodymium ions, luminescence of an excessive number of  $Eu^{3+}$  must be observed. This assumption was checked by synthesizing samples of  $LuBO_3$  doped with 1 at.% of Pr and 1 at.% of Eu, 1 at.% of Pr and 2 at.% of Eu, as well as 1 at.% of Pr and 3 at.% of Eu. All the three samples, according to the X-ray diffraction analysis data (Table 1), have a calcite structure. According to the aforesaid

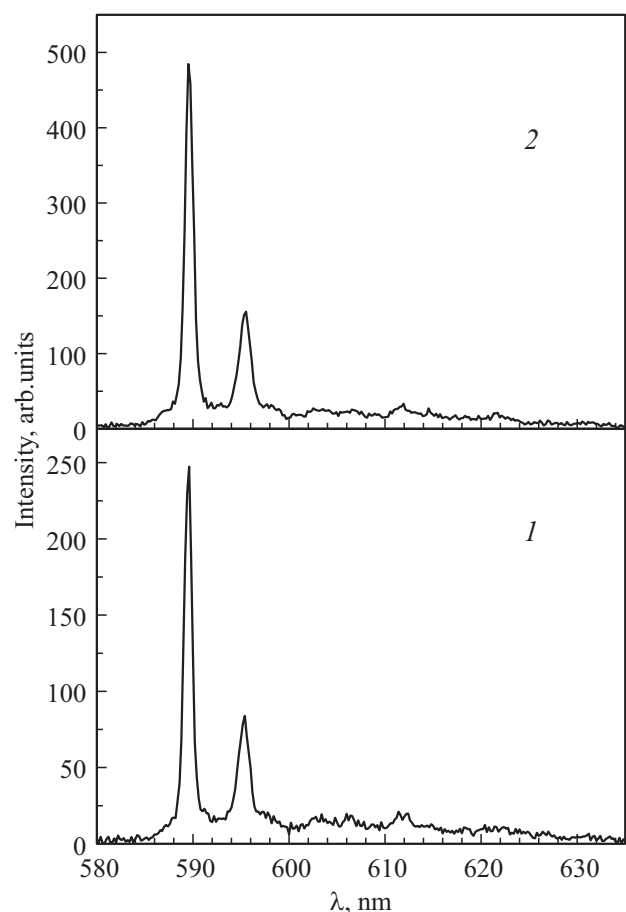


**Figure 6.** Luminescence spectra for  $Pr_{0.99-x-y}Lu_xEu_yBO_3$  orthoborates. 1 —  $x = 0.97$ ,  $y = 0.02$ ; 2 —  $x = 0.96$ ,  $y = 0.03$ .



assumption, luminescence is not observed in the samples of  $\text{Pr}_{0.01}\text{Lu}_{0.98}\text{Eu}_{0.01}\text{BO}_3$ , but luminescence of  $\text{Eu}^{3+}$  ions is observed in  $\text{Pr}_{0.01}\text{Lu}_{0.97}\text{Eu}_{0.02}\text{BO}_3$  and  $\text{Pr}_{0.01}\text{Lu}_{0.96}\text{Eu}_{0.03}\text{BO}_3$  orthoborates whose luminescence spectra and luminescence excitation spectra are shown in Fig. 6, spectra 1, 2 and Fig. 7, spectra 1, 2. The most intensive bands in the luminescence spectra for these samples are the bands with  $\lambda_{\text{max}} = 589.8$  and  $595.7$  nm (electron transition  ${}^5\text{D}_0 \rightarrow {}^7\text{F}_1$ ), typical for the calcite modification  $\text{LuBO}_3(\text{Eu})$  [1,37,38]. The ultraviolet region of the excitation spectra of the most intensive luminescence band (589.8 nm) features a wide band with the maximum at  $\lambda_{\text{ex}} = 254$  nm, which corresponds to a charge transfer band (CTB) [1,3,39]. The band with  $\lambda_{\text{ex}} = 394$  nm (electron transition  ${}^7\text{F}_0 \rightarrow {}^5\text{L}_6$ ), corresponding to resonant excitation of  $\text{Eu}^{3+}$  ions, is more than  $\sim 40$  times smaller than the CTB (Fig. 7, spectra 1, 2), which is typical for the calcite modification  $\text{LuBO}_3(\text{Eu})$  [1,3,13,14].

It should be noted that the number of excess  $\text{Eu}^{3+}$  ions in relation to  $\text{Pr}^{3+}$  ions in the samples of  $\text{Pr}_{0.01}\text{Lu}_{0.96}\text{Eu}_{0.03}\text{BO}_3$  (sample 2) is 2 times greater than in the samples of  $\text{Pr}_{0.01}\text{Lu}_{0.97}\text{Eu}_{0.02}\text{BO}_3$  (sample 1). Therefore, if a charge

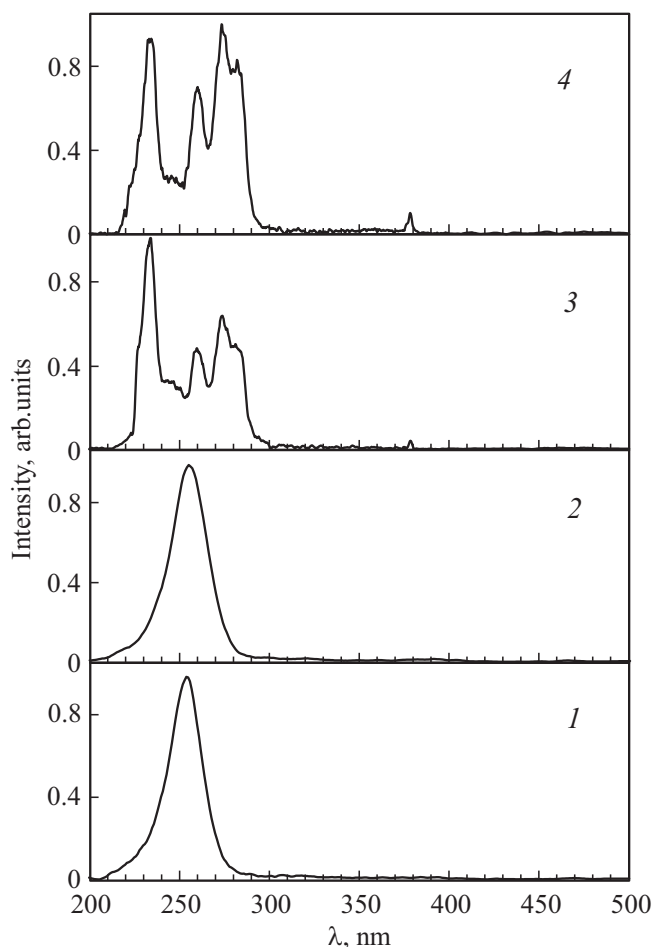


**Figure 7.** Luminescence excitation spectra for  $\text{Pr}_{1-x-y-z}\text{Lu}_x\text{Eu}_y\text{Tb}_z\text{BO}_3$  orthoborates. 1 —  $x = 0.97$ ,  $y = 0.02$ ,  $z = 0$ ; 2 —  $x = 0.96$ ,  $y = 0.03$ ,  $z = 0$ ; 3 —  $x = 0.96$ ,  $y = 0$ ,  $z = 0.02$ ; 4 —  $x = 0.94$ ,  $y = 0$ ,  $z = 0.04$ .

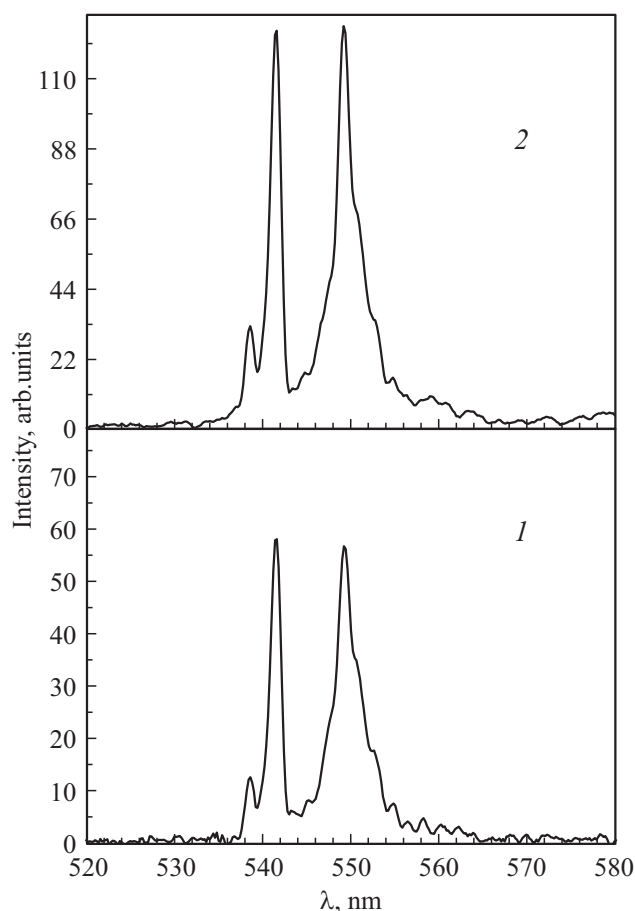


**Figure 8.** Luminescence spectra for  $\text{Pr}_{0.99-x-z}\text{Lu}_x\text{Tb}_z\text{BO}_3$  orthoborates. 1 —  $x = 0.96$ ,  $z = 0.02$ ; 2 —  $x = 0.94$ ,  $z = 0.04$ .

is transferred from  $\text{Pr}^{3+}$  to  $\text{Eu}^{3+}$  in these compounds, luminous intensity of  $\text{Eu}^{3+}$  ions in sample 2 must be 2 times greater than in sample 1. The experiment confirms this conjecture. The ratios of intensities of the most intensive bands with  $\lambda_{\text{max}} = 589.8$  and  $595.7$  nm in the spectra of samples 2 and 1 are equal to  $\sim 2$  and  $\sim 1.9$  respectively (Fig. 6, spectra 1 and 2). This additionally confirms the aforesaid conjecture that a charge transfer from  $\text{Pr}^{3+}$  ions to  $\text{Eu}^{3+}$  ions (MMCT) indeed takes place. Luminescence of  $\text{Eu}^{3+}$  ions during the MMCT process can be observed only in samples where concentration of  $\text{Eu}^{3+}$  ions is more than concentration of  $\text{Pr}^{3+}$  ions. This circumstance explains the absence of luminescence in  $\text{Pr}_{0.99-x}\text{Lu}_x\text{Eu}_{0.01}\text{BO}_3$  orthoborates with  $0 \leq x \leq 0.98$ .

It is interesting to study the spectral characteristics of  $\text{Pr}_{1-z}\text{Lu}_{x-z}\text{Tb}_z\text{BO}_3$  orthoborates where  $\text{Tb}^{3+}$  ions are optically active. The luminescence excitation spectra and luminescence spectra for the most intensive luminescence bands of  $\text{Pr}_{0.02}\text{Lu}_{0.96}\text{Tb}_{0.02}\text{BO}_3$  (sample 3) and  $\text{Pr}_{0.02}\text{Lu}_{0.94}\text{Tb}_{0.04}\text{BO}_3$  orthoborates (sample 4), which have, according to the X-ray diffraction analysis data, a calcite structure (Table 1) are shown in Fig. 7 and Fig. 8 respectively.

The luminescence excitation spectrum for samples 3 and 4 has four bands in the short-wave spectrum region with  $\lambda_{\text{ex}} \sim 235, 260, 274$  and  $283$  nm (transition  $4f^8 \rightarrow 4f^75d^1$ ) and a narrow resonance band with  $\lambda_{\text{ex}} = 378$  nm ( ${}^7\text{F}_6 \rightarrow {}^5\text{D}_3$ ) (Fig. 8, spectrum 1). This spectrum is typical for luminescence of terbium in the calcite modification  $\text{LuBO}_3(\text{Tb})$  [1,4,13]. The most intensive bands in the luminescence spectrum for the samples of  $\text{Pr}_{0.02}\text{Lu}_{0.96}\text{Tb}_{0.02}\text{BO}_3$  and  $\text{Pr}_{0.02}\text{Lu}_{0.94}\text{Tb}_{0.04}\text{BO}_3$  are the luminescence bands, typical for the calcite modification  $\text{LuBO}_3(\text{Tb})$ , with  $\lambda_{\text{max}} = 541.8$  and  $549.5$  nm ( ${}^5\text{D}_4 \rightarrow {}^7\text{F}_5$ ), the amplitudes of which are comparable (Fig. 8, spectra 1, 2) [1,4,13]. Luminous intensity of samples 3 and 4 is proportional to concentration of Tb ions in the samples: in sample 4 it is  $\sim 2$  times higher than in sample 3. We might expect luminescence of terbium ions to occur in  $\text{Pr}_{0.98-x}\text{Lu}_x\text{Tb}_{0.02}\text{BO}_3$  orthoborates when concentration of Pr ions is considerably higher than 2 at.%. However, luminescence of  $\text{Tb}^{3+}$  ions is not present in the samples containing 98 and 28 at.% of Pr. Possibly, since Tb may have the valency 2+, 3+ and 4+ [32], a charge transfer from  $\text{Pr}^{3+}$  to  $\text{Tb}^{3+}$  also takes place at higher concentrations of  $\text{Pr}^{3+}$  ions, which results in quenching of terbium ions luminescence. Thus, luminescence of  $\text{Eu}^{3+}$  ions is observed in  $\text{Pr}_{1-x}\text{Lu}_x\text{BO}_3(\text{Eu})$  orthoborates where concentration of  $\text{Eu}^{3+}$  ions is higher than concentration of  $\text{Pr}^{3+}$  ions. Luminescence of  $\text{Tb}^{3+}$  ions is observed in the samples of  $\text{LuBO}_3(\text{Pr}, \text{Tb})$  containing 2 at.% of  $\text{Pr}^{3+}$  and 2 at.% of  $\text{Tb}^{3+}$ , but is absent in  $\text{Pr}_{0.98-x}\text{Lu}_x\text{Tb}_{0.02}\text{BO}_3$  orthoborates with  $0.7 \geq x \geq 0$ .

## 7. Conclusion

The present paper is dedicated to studying the structure, morphology, IR spectra of  $\text{Pr}_{0.99-x}\text{Lu}_x\text{Eu}_{0.01}\text{BO}_3$  orthoborates with  $0 \leq x \leq 0.99$  synthesized at  $970^\circ\text{C}$ .

We have established a one-to-one correspondence between the structural modification and IR spectra of these compounds.

Five regions of  $\text{Lu}^{3+}$  concentrations, where certain structural states exist, can be distinguished in  $\text{Pr}_{0.99-x}\text{Lu}_x\text{Eu}_{0.01}\text{BO}_3$  orthoborates.

With  $0 \leq x \leq 0.1$ , the  $\text{Pr}_{0.99-x}\text{Lu}_x\text{Eu}_{0.01}\text{BO}_3$  orthoborates are single-phase with an aragonite structure (space group  $Pnma$ ). The IR spectra have the absorption bands  $594, 615, 717, 791, 947$  and  $1306$   $\text{cm}^{-1}$  which correspond to the aragonite phase  $\text{PrBO}_3$ .

With  $0.1 < x < 0.6$  the samples are two-phase — they contain aragonite and vaterite phases. The IR spectra have the bands typical for aragonite and vaterite structures.

With  $0.6 < x \leq 0.8$  the compounds become single-phase with a vaterite structure (space group  $P6_3/mmc$ ). The IR spectra have the absorption bands  $569, 712, 876, 933$  and  $1088$   $\text{cm}^{-1}$ , typical for orthoborates with a vaterite structure.

With  $0.8 < x \leq 0.95$  the samples are two-phase — they contain vaterite and calcite phases. The IR spectra have the bands typical for the vaterite and calcite modifications of these samples.

With  $0.95 < x < 0.99$  the orthoborates are single-phase with a calcite structure (space group  $R\bar{3}c$ ). The IR spectra contain the absorption bands  $631, 748, 773, 1242$   $\text{cm}^{-1}$  typical for orthoborates with a calcite structure.

It is shown that luminescence of  $\text{Eu}^{3+}$  ions is observed in the samples of  $\text{LuBO}_3(\text{Pr}, \text{Eu})$  where europium concentration exceeds praseodymium concentration.

Thus, the three types of crystalline phases: aragonite, vaterite and calcite successively change each other (as lutetium concentration increases) in  $\text{Pr}_{0.99-x}\text{Lu}_x\text{Eu}_{0.01}\text{BO}_3$  orthoborates synthesized at  $970^\circ\text{C}$ , like in  $\text{La}_{0.98-x}\text{Lu}_x\text{Eu}_{0.02}\text{BO}_3$  compounds.

## Funding

The work has been performed under the state assignment of ISSP of RAS.

The authors would like to thank the Research Facility Center of ISSP of RAS for the morphology study of the samples and their characterization by IR spectroscopy and X-ray diffraction analysis methods.

## Conflict of interest

The authors declare that they have no conflict of interest.

## References

- [1] C. Mansuy, J.M. Nedelec, C. Dujardin, R. Mahiou. *Opt. Mater.* **29**, 6, 697 (2007).
- [2] Jun Yang, Chunxia Li, Xiaoming Zhang, Zewei Quan, Cuimiao Zhang, Huaiyong Li, Jun Lin. *Chem. Eur. J.* **14**, 14, 4336 (2008).
- [3] Y.H. Zhou, J. Lin, S.B. Wang, H.J. Zhang. *Opt. Mater.* **20**, 1, 13 (2002).
- [4] J. Yang, G. Zhang, L. Wang, Z. You, S. Huang, H. Lian, J. Lin. *J. Solid State Chem.* **181**, 12, 2672 (2008).
- [5] S.Z. Shmurak, V.V. Kedrov, A.P. Kiselev, T.N. Fursova, I.I. Zverkova. *FTT* **62**, 12, 2110 (2020) (in Russian).
- [6] E.M. Levin, R.S. Roth, J.B. Martin. *Am. Miner.* **46**, 9–10, 1030 (1961).
- [7] J. Hölsä, *Inorg. Chim. Acta* **139**, 1–2, 257 (1987).
- [8] G. Chadeyron, M. El-Ghozzi, R. Mahiou, A. Arbus, C. Cousseins. *J. Solid State Chem.* **128**, 261 (1997).
- [9] D. Santamaría-Pérez, O. Gomis, J. Angel Sans, H.M. Ortiz, A. Vegas, D. Errandonea, J. Ruiz-Fuertes, D. Martínez-García, B. García-Domene, Andréé L.J. Pereira, F. Javier Manjoón, P. Rodríguez-Hernández, A. Muñoz, F. Piccinelli, M. Bettinelli, C. Popescu. *J. Phys. Chem. C* **118**, 4354 (2014).
- [10] Wen Ding, Pan Liang, Zhi-Hong Liu. *Mater. Res. Bull.* **94**, 31 (2017).
- [11] Wen Ding, Pan Liang, Zhi-Hong Liu. *Solid State Sci.* **67**, 76 (2017).
- [12] S.Z. Shmurak, V.V. Kedrov, A.P. Kiselev, I.M. Shmytko. *FTT* **57**, 1, 19 (2015) (in Russian).

- [13] S.Z. Shmurak, V.V. Kedrov, A.P. Kiselev, T.N. Fursova, I.M. Shmytko. *FTT* **57**, 8, 1558 (2015) (in Russian).
- [14] S.Z. Shmurak, V.V. Kedrov, A.P. Kiselev, T.N. Fursova, I.I. Zverkova, E.Yu. Postnova. *FTT* **63**, 7, 933 (2021) (in Russian).
- [15] S.Z. Shmurak, V.V. Kedrov, A.P. Kiselev, T.N. Fursova, I.I. Zverkova, E.Yu. Postnova. *FTT* **63**, 10, 1615 (2021) (in Russian).
- [16] S.Z. Shmurak, V.V. Kedrov, A.P. Kiselev, T.N. Fursova, I.I. Zverkova, S.S. Khasanov. *FTT* **63**, 12, 2142 (2021) (in Russian).
- [17] R.S. Roth, J.L. Waring, E.M. Levin. *Proc. 3rd Conf. Rare Earth Res. Clearwater, Fla.* (1964). P. 153.
- [18] I.M. Shmytko, I.N. Kiryakin, G.K. Strukova. *FTT* **55**, 7, 1369 (2013) (in Russian).
- [19] N.I. Steblevskaya, M.I. Belobeletskaya, M.A. Medkov. *Zhurn. neorgan. khimii* **66**, 4, 440 (2021) (in Russian).
- [20] J. Guang, C. Zhang, C. Wang, L. Liu, C. Huang, S. Ding. *Cryst. Eng. Commun.* **14**, 579 (2012).
- [21] J. Zhang, M. Yang, H. Jin, X. Wang, X. Zhao, X. Liu, L. Peng. *Mater. Res. Bull.* **47**, 247 (2012).
- [22] Heng-Wei Wei, Li-Ming Shao, Huan Jiao, Xi-Ping Jing. *Opt. Mater.* **75**, 442 (2018).
- [23] R. Nayar, S. Tamboli, A.K. Sahu, V. Nayar, S.J. Dhoble. *J. Fluoresc.* **27**, 251 (2017).
- [24] S.K. Omanwar, N.S. Savala. *Appl. Phys. A* **123**, 673 (2017).
- [25] C. Badan, O. Esenturk, A. Yelmaz. *Solid State Sci.* **14**, 11–12, 1710 (2012).
- [26] C.E. Weir, E.R. Lippincott. *J. RES. Natl. Bur. Std.-A. Phys. Chem.* **65A**, 3, 173 (1961).
- [27] A. Szczeszak, T. Grzyb, St. Lis, R.J. Wiglusz. *Dalton Transactions* **41**, 5824 (2012).
- [28] Ling Li, Shihong Zhou, Siyuan Zhang. *Solid State Sci.* **10**, 1173 (2008).
- [29] A. Haberer, R. Kaindl, H.Z. Huppertz. *Naturforsch. B* **65**, 1206 (2010).
- [30] R. Velchuri, B.V. Kumar, V.R. Devi, G. Prasad, D.J. Prakash, M. Vital. *Mater. Res. Bull.* **46**, 8, 1219 (2011).
- [31] Jin Teng-Teng, Zhang Zhi-Jun, Zhang Hui, Zhao Jing-Tai. *J. Inorganic Mater.* **28**, 10, 1153 (2013).
- [32] A.G. Ryabukhin. *Izv. Chelyabinskogo nauch. tsentra* **4**, 33 (2000) (in Russian).
- [33] J.P. Laperches, P. Tarte. *Spectrochim. Acta* **22**, 1201 (1966).
- [34] C.E. Weir, R.A. Schroeder. *J. RES. Natl. Bur. Std.-A. Phys. Chem.* **68A**, 5, 465 (1964).
- [35] G. Blasse. *A. Bril. J. Chem. Phys.* **47**, 6, 1920 (1967).
- [36] G. Blasse. *Phys. Status Solidi A* **75**, 1, K41 (1983).
- [37] J. Yang, G. Zhang, L. Wang, Z. You, S. Huang, H. Lian, J. Lin. *J. Solid State Chem.* **181**, 12, 2672 (2008).
- [38] G. Blasse, B.C. Grabmaier. *Luminescent Materials*. Springer-Verlag, Berlin–Heidelberg (1994). 233 p.
- [39] D. Hrrniak, E. Zych, L. Kepinski, W. Streck. *J. Phys. Chem. Solids* **64**, 1, 11 (2003).